NEOPLASIA
www.neoplasia.com

Volume 13 Number 4 April 2011 pp. 327–338 327

Synergy of Nab-paclitaxel and Bevacizumab in Eradicating Large Orthotopic Breast Tumors and Preexisting Metastases[1,2]

Lisa D. Volk*, Michael J. Flister*, Deena Chihade*, Neil Desai†, Vuong Trieu† and Sophia Ran*

*Department of Medical Microbiology, Immunology and Cell Biology, Southern Illinois University School of Medicine, Springfield, IL, USA; †Abraxis Bioscience, Inc, Marina del Rey, CA, USA

Abstract

INTRODUCTION: Patients with metastatic disease are considered incurable. We previously showed that nab-paclitaxel (nanoparticle albumin-embedded paclitaxel) combined with anti–vascular endothelial growth factor A (VEGF-A) antibody, bevacizumab, eradicates orthotopic small-sized breast tumors and metastasis. Here, we assessed this therapy in two models of advanced (450-600 mm^3) breast tumors and delineated VEGF-A–dependent mechanisms of tumor resistance. *METHODS:* Mice with luciferase-tagged advanced MDA-MB-231 and MDA-MB-435 tumors were treated with saline, nab-paclitaxel (10 or 30 mg/kg), bevacizumab (4 mg/kg), or combined drugs. Lymphatic and lung metastases were measured by luciferase assay. Proinflammatory and survival pathways were measured by ELISA, Western blot and immunohistochemistry. *RESULTS:* Nab-paclitaxel transiently suppressed primary tumors by 70% to 90% but had no effect on metastasis. Coadministration of bevacizumab increased the response rate to 99%, including 71% of complete responses in MDA-MB-231–bearing mice treated concurrently with 30 mg/kg of nab-paclitaxel. This combinatory regimen significantly reduced or eliminated preexisting lymphatic and distant metastases in MDA-MB-231 and MDA-MB-435 models. The mechanism involves paclitaxel-induced NF-κB pathway that upregulates VEGF-A and other tumor prosurvival proteins. *CONCLUSIONS:* Bevacizumab prevents tumor recurrence and metastasis promoted by nab-paclitaxel activation of NF-κB pathway. Combination therapy with high-dosed nab-paclitaxel demonstrates the potential to eradicate advanced primary tumors and preexisting metastases. These findings strongly support translating this regimen into clinics.

Neoplasia (2011) 13, 327–338

Introduction

Chemotherapy is a frontline treatment of breast and other epithelial malignancies, particularly those that are not resectable. Treatment of measurable tumors with chemotherapeutic drugs results in three outcomes: no response occurring in 5% to 10% of breast cancer (BC) patients [1,2], a complete response (CR) occurring in 10% to 20% of patients [1,2], and a partial response (PR) defined as more than 50% of the tumor reduction in response to therapy [1]. PR is the most common outcome with 50% occurrence in patients in the neoadjuvant setting with noninvasive BC [1] and higher frequency in patients with metastatic disease, triple-negative, and therapy-resistant tumors [3]. Incomplete responsiveness to cytotoxic drugs is one of the main reasons for increased mortality due to uncontrolled tumor growth. Delineating the mechanisms underlying PR holds the promise to identify the reasons for tumor resistance to chemotherapy and the potential to improve the efficacy of anticancer drugs.

Abbreviations: ABX, Abraxane, or paclitaxel protein-bound particles for injectable suspension, also abbreviated as nab-paclitaxel; Bev, bevacizumab, humanized anti–human VEGF-A antibody, also known as Avastin; BC, breast cancer; i.p., intraperitoneally; i.v., intravenously; ILN, ipsilateral lymph node; LN, lymph node; MFP, mammary fat pad; MTD, maximal tolerated dose; (p)-, phosphorylated form of protein; PBS, phosphate-buffered saline; PBST, PBS containing Tween-20; RLU, relative light unit; TGD, tumor growth delay; VEGF-A, vascular endothelial growth factor-A

Address all correspondence to: Sophia Ran, PhD, Department of Medical Microbiology, Immunology and Cell Biology, Southern Illinois University School of Medicine, Springfield, IL 62794-9626. E-mail: sran@siumed.edu

[1]This work was supported, in part, by a research grant from Abraxis Bioscience, Inc, Los Angeles, CA; the National Institutes of Health (No. 1R01-CA140732-01A1), Illinois William E. McElroy Foundation; and the Department of Defense Breast Cancer Research Program (No. BC086079) awarded to Sophia Ran. Two contributors to this work, Neil Desai and Vuong Trieu, are employed by Abraxis Bioscience, Inc. Lisa Volk, Deena Chihade, and Michael Flister declare no competing interests.

[2]This article refers to supplementary materials, which are designated by Table W1 and Figures W1 to W3 and are available online at www.neoplasia.com.

Received 29 October 2010; Revised 25 January 2011; Accepted 27 January 2011

DOI 10.1593/neo.101490

One of the reasons for tumor chemoresistance is overexpression of P-glycoproteins that pump out cytotoxic drugs, thus preventing intracellular accumulation of the lethal dose [4]. Another mechanism is mediated by vascular endothelial growth factor A (VEGF-A), an angiogenic factor [5,6] that protects tumor cells from apoptosis through autocrine activation of VEGF-A receptors expressed on tumor cells [7]. VEGF-A is upregulated by various chemodrugs including paclitaxel [8], docetaxel [8], carboplatin [9], cisplatin [10], 5-fluorouracil [11], dacarbazine [12], and anthracyclines [13]. Although the mechanism by which these drugs elicit VEGF-A expression is unclear, it might occur through activation of NF-κB [14] and PI3K/AKT pathways [15] that are induced by chemotherapy in both malignant [10,11] and endothelial cells [9]. The crucial role of VEGF-A in chemoresistance was shown in both preclinical [16,17] and clinical studies [18,19] demonstrating superior efficacy of chemodrugs when combined with anti–VEGF-A antibody. In particular, the combination of the anti–VEGF-A antibody, bevacizumab, with 5-fluorouracil, leucovorin, oxaliplatin, or irinotecan, showed an additive or synergistic effect [17]. The E2100 trial also showed that paclitaxel/bevacizumab therapy increased a response rate and significantly prolonged patient survival compared with paclitaxel treatment alone [20,21]. In addition, bevacizumab combined with other taxanes improved the outcome in patients with ovarian tumors, although this benefit was short-lived [18].

Of various taxanes, paclitaxel, a microtubule-stabilizing cytotoxic agent, is widely used against metastatic and refractory tumors [22]. The clinical use of Cremophor-based paclitaxel (Taxol) has been recently improved by formulating it as Cremophor-free, albumin-bound 130-nm nanoparticles coined nab-paclitaxel or Abraxane [23,24]. Nab-paclitaxel demonstrated several advantages over Cremophor-based paclitaxel in clinical [22,25] and experimental [26,27] studies owing to albumin encapsulation of the active component allowing for delivery of a high dose of paclitaxel without the use of solvent [28]. This leads to dose-proportional pharmacokinetics, higher maximal tolerated dose (MTD), and improved efficacy [22,29]. Nab-paclitaxel treatment of metastatic BC patients demonstrated a higher response rate and longer time to progression when compared with Cremophor-based drug [28,29]. The superior efficacy of nab-paclitaxel *versus* conventional paclitaxel was also shown in preclinical xenograft models demonstrating increased incidence of tumor regressions, longer time to recurrence, and extended survival [26]. These advantages are related to the improved delivery of nab-paclitaxel compared with solvent-based paclitaxel, leading to 33% increased intratumoral concentrations and doubling of the MTD [26].

We recently demonstrated that nab-paclitaxel efficacy is further improved by coadministration of anti–VEGF-A antibody [16]. It was shown that combined nab-paclitaxel/bevacizumab therapy eradicated small-sized (150-200 mm^3) orthotopic breast tumors in 40% of the mice and reduced metastatic incidence [16]. Whereas these results were encouraging, the models of small-sized tumors may not adequately reflect the clinical challenges in patients who present with advanced tumor burden and preexisting metastases. In the present study, we allowed luciferase-tagged MDA-MB-231-Luc$^+$ and MDA-MB-435-Luc$^+$ tumors to reach 450 to 600 mm^3 before initiating treatment. In these tumor models, 100% of the animals exhibited preexisting metastases in both lung and lymph nodes (LN). The results showed that bevacizumab combined with nab-paclitaxel at 10- and 30-mg/kg doses eradicated large 231-Luc$^+$ tumors in 33% and 71% of mice, respectively. Although no complete eradications were achieved in the 435-Luc$^+$ model, the combined treatment resulted in 94% tumor inhibition and prolonged time to progression for more than 80 days. Importantly, in both models, the combined therapy substantially decreased the incidence and the burden of preexisting pulmonary and lymphatic metastases. Collectively, these data suggest that the combination of bevacizumab and nab-paclitaxel can be effective in eradicating advanced tumors and preexisting metastases in human cancer patients.

Materials and Methods

Materials

Dulbecco modified Eagle medium and standard additives were obtained from Lonza (Basel, Switzerland). Ketamine and xylazine were from Phoenix Scientific (St Joseph, MO). Endotoxin-free sterile 150 mM NaCl solution (saline) and protease inhibitors were from Sigma (St Louis, MO). Matrigel was from BD Bioscience (Franklin Lakes, NJ).

Antibodies

Primary rabbit anti–Bcl-xL, anti-Akt, anti–p-Akt, anti-p44/42, anti–p-p44/42 anti-p50, anti–p-p50, anti-p65, anti–p p65, anti–VEGF-A, and anti–Bcl-2 antibodies were from Cell Signaling (Danvers, MA) and Thermo Scientific (Waltham, MA). Mouse–anti–β-actin (JLA20) was from Developmental Studies Hybridoma Bank (Iowa City, IA). Antirabbit and antimouse secondary antibodies were from Jackson ImmunoResearch (West Grove, PA).

Study Drugs

Paclitaxel albumin-bound particles for injectable suspension (nab-paclitaxel; Abraxane) was obtained from Abraxis BioScience (Los Angeles, CA). Drugs were reconstituted in saline, prepared fresh daily, and given within 1 hour of preparation. Bevacizumab (Avastin), humanized anti–VEGF-A antibody, manufactured by Genentech (San Francisco, CA), was obtained from a local pharmacy.

Human MDA-MB-231 and MDA-MB-435 Carcinoma Cell Lines and Their Luciferase Derivatives

Luciferase-tagged subline of MDA-MB-231, designated 231-Luc$^+$, has been extensively characterized in previous studies [16,30]. Luciferase-tagged MDA-MB-435 subline, designated 435-Luc$^+$, was a generous gift from Dr Sierra (Universitaria de Bellvitge, Barcelona, Spain) and described elsewhere [16,31]. Cells were cultured in Dulbecco modified Eagle medium supplemented with 5% fetal bovine serum and standard additives and were subcultured by using 0.5 mM EDTA diluted in phosphate-buffered saline (PBS).

Mouse Orthotopic Models of Human BC

Orthotopic 231-Luc$^+$ and 435-Luc$^+$ tumor models were previously described [16,30]. Briefly, 4×10^6 cells suspended in 50% Matrigel were implanted into the mammary fat pad (MFP) of 4- to 6-week-old female SCID mice (National Cancer Institute, Frederick, MD). Every 2 to 3 days, perpendicular tumor diameters were measured by digital caliper and used to calculate tumor volume according to the formula: volume = $Dd^2\pi/6$, where D indicates the larger diameter and d indicates the smaller diameter. Animal care was in accordance with institutional guidelines.

Treatment with Nab-paclitaxel and Bevacizumab

Mice bearing advanced 231-Luc$^+$ or 435-Luc$^+$ tumors (450-600 mm^3) were randomized into groups (7-16 per group) and treated with saline (control), nab-paclitaxel alone (10 or 30 mg/kg, intravenously [i.v.], daily for five consecutive days), bevacizumab alone (4 mg/kg, intraperitoneally [i.p.], biweekly), or nab-paclitaxel combined with bevacizumab. Nab-paclitaxel course was repeated twice with one rest week between the courses. Bevacizumab treatment consisting of 4-mg/kg dose in saline (0.1 ml) injected i.p., biweekly, for the study's duration, began 24 hours after the first nab-paclitaxel injection. Control group received saline (0.1 ml), injected i.v. or i.p. on the same days as nab-paclitaxel and bevacizumab treatments, respectively. Mice were killed when tumor volumes in the control group reached 1800 mm^3. Metastasis was measured by luciferase activity in tissue extracts of the axillary, brachial, inguinal LNs, and lungs.

Time Course of Metastatic Progression

Mice with orthotopic 231-Luc$^+$ tumors were randomized into groups (n = 4-8) and killed when average tumor volumes reached 100, 150, 250, 500, 1000, and 1800 mm^3. Metastasis was determined by measuring luciferase in tissues extracts of ipsilateral and contralateral LNs, lung, brain, heart, kidney, MFP, and ovaries.

Optimization of the Combined Nab-paclitaxel/Bevacizumab Regimen

Mice with orthotopic 435-Luc$^+$ tumors were randomized into four groups (n = 8 per group) when tumor volume reached 450 mm^3. Group 1 received saline; group 2 was treated with three courses of nab-paclitaxel (10 mg/kg) followed by bevacizumab administrated after cessation of chemotherapy; group 3 was concurrently treated with nab-paclitaxel and bevacizumab, with both drugs being discontinued on cessation of chemotherapy; and group 4 was concurrently treated with nab-paclitaxel and bevacizumab with continued bevacizumab treatment for the study's duration. Nab-paclitaxel was administered for three courses with one rest week between courses. Bevacizumab was administered biweekly (i.p.) at 4 mg/kg. The study was terminated 40 days after the third nab-paclitaxel course.

Determination of Metastatic Burden

Luciferase activity was determined as previously described [16]. Briefly, tissues were homogenized in ice-cold cell culture lysis reagent buffer (Promega, Madison, WI) containing protease inhibitors. Luciferase Assay Reagent (50 μl) was mixed with lysates (10 μl) followed by luminescence detection using a luminometer (Berthold, Germany). Luminescence of buffer alone was subtracted from the results. Data are expressed as relative light units (RLUs) normalized per milligram of protein. Extracts with luminescence of 800 RLUs above background were rated as positive for metastasis.

Analysis of Cytokine Production Stimulated by Nab-paclitaxel

231-Luc$^+$ cells were seeded at a density of 4 × 10^5 per well and treated with 2.5, 5, 7.5, 10, or 30 nM of nab-paclitaxel for 72 hours, followed by collection of the conditioned medium. Cytokines were measured using the Linco High Sensitivity Human Cytokine Kit (Millipore, Billerica, MA) according to the manufacturer's instructions. Plates were quantified using the Luminex-100 system with Beadview software version 1.7 (Luminex, Austin, TX). Cytokine production was expressed as picograms per milliliter or nanograms per milliliter normalized per 1 × 10^6 cells. Each experimental condition was tested in triplicate and reproduced in two separate experiments.

Western Blot Analysis

Equal protein amounts of lysates from individual mice were combined per group for Western blot analysis of 231-Luc$^+$ tumors. Lysates of 231-Luc$^+$ cells treated with 0, 2.5, 5, 10, or 30 nM nab-paclitaxel were harvested after 8, 24, and 48 hours in lysis buffer (50 mM Tris-HCl, pH 7.5, 150 mM NaCl, 1 mM EDTA, 1% Triton X-100, 0.1% SDS, phosphatase, and protease inhibitors). Proteins were separated in 10% to 12% SDS–polyacrylamide gel and transferred onto nitrocellulose membranes followed by overnight incubation with primary antibodies against NF-κB p50, p-p50, NF-κB p65, p-p65, p44/42, p-p44/42, Akt, p-Akt, Bcl-xL, Bcl-2, and β-actin. Membranes were incubated for 1 hour with HRP-conjugated secondary antibody before development with ECL (Pierce, Rockford, IL). Protein bands were visualized using a Fujifilm LAS-3000 camera (Fujifilm, Valhalla, NY), and densitometry was analyzed with Image-Reader LAS-3000 software (Valhalla, NY).

Immunohistochemistry

Frozen sections were fixed with 2% paraformaldehyde for 30 minutes and postfixed with ice-cold methanol. After rehydration in PBS containing Tween-20 (PBST), sections were incubated for 2 hours with primary antibodies (1:100 in PBST containing 0.5% bovine serum albumin), washed for 10 minutes in PBST, followed by 1-hour incubation with Cy3-conjugated antirabbit secondary antibodies. Slides were mounted with Vectashield containing 4′,6-diamidino-2-phenylindole (Vector Laboratories, Burlingame, CA). Images were acquired at a constant exposure on a DP71 camera mounted on an Olympus BX41 microscope using DP Controller software (Olympus, Center Valley, PA).

Fluorescent Intensity Measurements

Tumors harvested from mice treated for 5 days with saline or nab-paclitaxel (10 mg/kg) were stained with anti–VEGF-A antibodies. To limit nonspecific background, a constant exposure was set to above the level of tissue staining with secondary antibodies alone. Pixels with intensity less than 3.6 were excluded from analysis as background. Fluorescent images were converted to 8-bit grayscale, and the mean fluorescent intensity of VEGF-A staining from control- and nab-paclitaxel–treated tumors (n = 3, 5 fields per section) ± SEM was calculated using the Plot Profile function of the ImageJ software (http://rsbweb.nih.gov/ij/). Plots of fluorescent staining intensity were generated using the 3D Interactive Surface Plot function of ImageJ.

Statistical Analysis

Statistical analysis was performed using SPSS 14.0 (SPSS, Chicago, IL). Results are expressed as mean ± SE. Statistically significant differences in tumor volume among experimental groups were determined by Student's t test. The synergistic effect of combined therapy was assessed using CompuSyn (CompuSyn, New York, NY), a software program based on the calculations for synergism developed by Chou et al. [32]. Statistically significant differences in incidence and burden of metastases were analyzed by nonparametric Fisher exact and Wilcoxon rank sum tests, respectively, because of the wide variability in metastatic burden among individual mice within the group. Metastatic burden values were log transformed and analyzed using variance test with

Tukey follow-up comparison to assess the relationship between tumor size and metastatic burden.

Results

Establishment of Advanced BC Model with Preexisting Metastases

Unlike situations in the clinics, most experimental studies are performed in animals bearing palpable or small-sized tumors with volume of 50 to 150 mm^3 (Table W1). The discrepancy between a relative tumor size in cancer patients and experimental animals at the time of the treatment might result in the significant difference in tumor response to therapy. To better model tumor responses in human patients, we performed all studies in mice bearing tumors of 500 mm^3 in volume. To determine the extent and distribution of metastases in the advanced 231-Luc$^+$ model, we measured kinetics of metastatic spread at different time points after tumor implantation. To this end, LNs and major visceral organs were harvested from mice (four to eight mice per group) bearing orthotopic 231-Luc$^+$ tumors of approximately 100, 150, 250, 500, 1000, and 1800 mm^3. Even at the earliest stage of tumor progression (tumor volume ~100 mm^3), most mice (75%) had already LN metastases. By the time tumors reached 250 mm^3, 100% of the mice had metastases in both LN and lungs (Figure 1 and Table 1). At the tumor volume of 485 mm^3, widespread distant metastasis was detected in the brain, heart, kidney, contralateral MFP, and ovary (Table 1). This kinetics demonstrates that therapies applied to tumors of 450 to 500 mm^3 target preexisting LNs and distant metastases rather than prevent their dissemination. Because all experiments in this study were performed in mice with tumors equal or larger than 500 mm^3, this model of advanced BC with preexisting metastases is much more akin to the clinical situation.

Nab-paclitaxel and Bevacizumab Act Synergistically to Suppress Tumor Growth in Orthotopic Models of Advanced BC

To analyze the effects of nab-paclitaxel/bevacizumab combination therapy, we used previously described luciferase-tagged orthotopic BC models, 231-Luc$^+$ and 435-Luc$^+$ [16,30]. Mice were treated with 10 mg/kg or the MTD of nab-paclitaxel in mice, 30 mg/kg [33]. Bevacizumab was administered i.p., 4 mg/kg, biweekly, for the experimental duration. Two independent experiments were performed using 231-Luc$^+$ and 435-Luc$^+$ models with 7 to 16 mice per group (Table 2).

The patterns of responses of 231-Luc$^+$ and 435-Luc$^+$ tumors were similar except that 435-Luc$^+$ tumors were more sensitive to VEGF-A depletion but more resistant to nab-paclitaxel than 231-Luc$^+$ tumors. Compared with the control group, bevacizumab alone inhibited growth of 435-Luc$^+$ tumors by 52% but had insignificant effect on

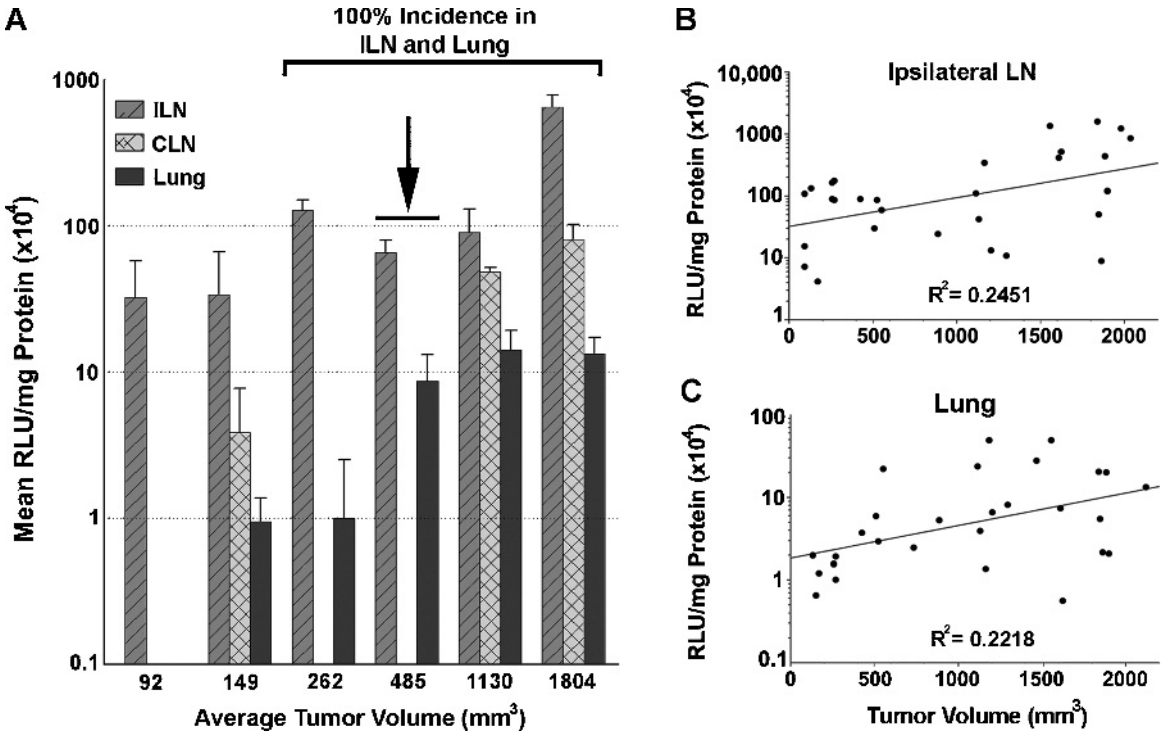

Figure 1. The kinetics of metastatic spread of orthotopic 231-Luc$^+$ tumors demonstrates preexisting metastases at the time of the treatment. Lymphatic and hematogenous metastasis was assessed in mice (n = 4 per group) bearing orthotopic 231-Luc$^+$ tumors killed when averaged tumors volumes ranged from 100 to 1800 mm^3. Metastatic incidence and burden were detected using firefly luciferase activity normalized to total mg of protein per organ of three ipsilateral LNs (ILNs) and one lobe of the lung. (A) The metastatic burden of the ILN and lung is presented as the mean luciferase activity per group ± SE. Note that 100% of mice bearing 231-Luc$^+$ tumors of volume equal or larger than 250 mm^3 had lymphatic and pulmonary metastases. The black arrow indicates tumor volume at which treatment began in experiments presented in Figures 2 and 3 depicted later. Luciferase measurements of lysates derived from ILN (B) and lung (C) of individual mice were plotted on a semilog graph as a function of tumor volume and subjected to linear regression analysis. Each dot represents tumor volume and its respective metastatic burden of an individual mouse as detected by luciferase activity. The squared Pearson correlation coefficient (R^2) derived from the linear regression analysis is shown on each graph.

Table 1. Incidence of Metastasis in 231-Luc$^+$ Model during Tumor Progression*.

Tumor Volume†	ILN‡	CLN‡	Lung	Brain	Heart	Kidney	cMFP‡	Ovary
92	3/4 (75%)	0/4 (0%)	0/4 (0%)	0/4 (0%)	1/4 (25%)	0/4 (0%)	0/4 (0%)	0/4 (0%)
149	1/4 (25%)	1/4 (25%)	3/4 (75%)	0/4 (0%)	1/4 (25%)	1/4 (25%)	1/4 (25%)	0/4 (0%)
262	4/4 (100%)	0/4 (0%)	4/4 (100%)	0/4 (0%)	0/4 (0%)	0/4 (0%)	1/4 (25%)	0/4 (0%)
485	4/4 (100%)	0/4 (0%)	4/4 (100%)	1/4 (25%)	1/4 (25%)	1/4 (25%)	2/4 (50%)	1/4 (25%)
1130	6/6 (100%)	2/7 (29%)	9/9 (100%)	1/4 (25%)	1/4 (25%)	1/4 (25%)	0/4 (0%)	0/4 (0%)
1804	10/10 (100%)	6/8 (75%)	9/9 (100%)	0/4 (0%)	3/4 (75%)	3/4 (75%)	2/4 (50%)	2/4 (50%)

Highlighted row indicates the average tumor volume at which treatment begins.

*Tissue lysates were from axillary, brachial, and inguinal LNs from the ipsilateral or contralateral sides, one lung, one lobe of the liver, whole brain, whole heart, ipsilateral kidney, and ovary, and contralateral MFPs were assayed for luciferase activity. Samples with readings greater than 800 light units per 10-μl lysate were considered positive. Background luminescence was less than 100 light units and was determined from tissue lysates from non–tumor-bearing mice. Results are presented as number of mice with positive organs per total number of mice at each average tumor size. Percentage of positive mice in each group is noted in parentheses.

†Average tumor volume in cubic millimeters.

‡ILN, CLN, and cMFP denote ipsilateral lymph nodes, contralateral lymph nodes, and contralateral mammary fat pad, respectively.

advanced 231-Luc$^+$ tumors (Figure 2, *A* and *C*). A low dose of nab-paclitaxel (10 mg/kg) suppressed growth of 435-Luc$^+$ and 231-Luc$^+$ tumors by 70% and 78%, respectively. A high dose of nab-paclitaxel (30 mg/kg) suppressed growth of 435-Luc$^+$ and 231-Luc$^+$ tumors by 92% and 82%, respectively (Figure 2, *B* and *D*; Table 2). Despite significant tumor suppression in both models by the 30-mg/kg dose, tumors recurred in all mice within 2 weeks after cessation of therapy and, by the end of experiments, approximated the size in saline-treated mice (Figure 2*D*).

The response to chemotherapy including reduced incidence of tumor recurrence was significantly improved in mice receiving both bevacizumab and nab-paclitaxel. In the groups receiving the 10-mg/kg dose, the extent of tumor inhibition was raised from 70% to 77% to 91% to 98%, and tumor growth delay (TGD) extended from 38 to 42 days to longer than 80 days. Significantly, 33% mice (2/7) with 231-Luc$^+$ tumors had CRs. Nab-paclitaxel at 30 mg/kg combined with bevacizumab raised the response rate to 99%. Within this group, 71% of mice (10/14) had complete tumor eradication. This was verified by palpation, gross observations, and assessment of residual luciferase activity in the tumor-implanted MFP. A high incidence of tumor eradication by the combined therapy was reproduced in two independent experiments (n = 14), both of which yielded statistically significant differences between nab-paclitaxel alone and the combined therapy, with P = .007 to P = .001 (Table 2). To assess whether the antitumor effect of the combined nab-paclitaxel and bevacizumab therapy was additive or synergistic, we used the CompuSyn software based on the calculations of synergy outlined by Chou et al. [32] for Taxol combined with other chemotherapeutic drugs. A comparison of tumor reduction by a singular drug *versus* combination therapy revealed a confidence interval of 0.002. On the basis of this software analysis, values less than 1 indicate the synergy between two drugs. Therefore, the antitumor effect of nab-paclitaxel and bevacizumab combined therapy is synergistic.

In summary, two courses of 30 mg/kg of nab-paclitaxel combined with bevacizumab inhibited advanced orthotopic 435-Luc$^+$ and 231-Luc$^+$ breast tumors by more than 90%, with complete eradication of

Table 2. The Effect of Bevacizumab and Nap-paclitaxel on Tumor Growth.

Treatment	n*	Drug Dose (mg/kg)	Mean Tumor Volume (mm^3)	% Inhibition of Control	TGD† *vs* Control	% CR‡	Statistical Significance§ *vs*	
							Control	ABX
MDA-MB-435 Luc$^+$								
Control	8	—	2157 ± 173	—	—	0	—	—
Bev¶	7	4	1030 ± 143	52.3	20	0	<.001	—
ABX¶	8	10	642 ± 110	70.2	38	0	<.001	—
ABX + Bev	7	10/04/11	174 ± 19	91.9	>80	0	<.001	<.001
Control	8	—	2151 ± 171	—	—	0	—	—
Bev	7	4	1030 ± 143	52.1	20	0	<.001	—
ABX	8	30	180 ± 15	91.7	>80	0	<.001	—
ABX + Bev	7	30/4	112 ± 33	94.8	>80	0	<.001	.05
MDA-MB-231 Luc$^+$								
Control	7	—	2095 ± 144	—	—	0	—	—
Bev	7	4	1332 ± 132	36.4	20	0	.006	—
ABX	7	10	469 ± 100	77.6	42	0	<.001	—
ABX + Bev	7	10/04/11	26 ± 17	98.8	>90	33.3	<.001	.001
Control	16	—	1973 ± 214	—	—	0	—	—
Bev	14	4	1933 ± 134	2.0	6	0	NS#	—
ABX	14	30	347 ± 59	82.4	55	0	<.001	—
ABX + Bev	14	30/4	12 ± 9	99.0	>90	71.4	<.001	<.001

*n indicates the number of mice per experimental group.

†TGD (tumor growth delay) is defined as a number of days that delayed the mean tumor volume per group reaching 1000 mm^3 compared with the saline-treated control group.

‡Complete response was defined as absence of palpable tumor at the original tumor injection site for the entire length of the experiments (90-95 days).

§Statistical significance was assessed using a Student's t test. P < .05 was considered to be significant.

¶Bev, ABX, and ABX + Bev denote treatment with bevacizumab, nab-paclitaxel, and combination of the two drugs, respectively.

#NS indicates that results were not statistically significant.

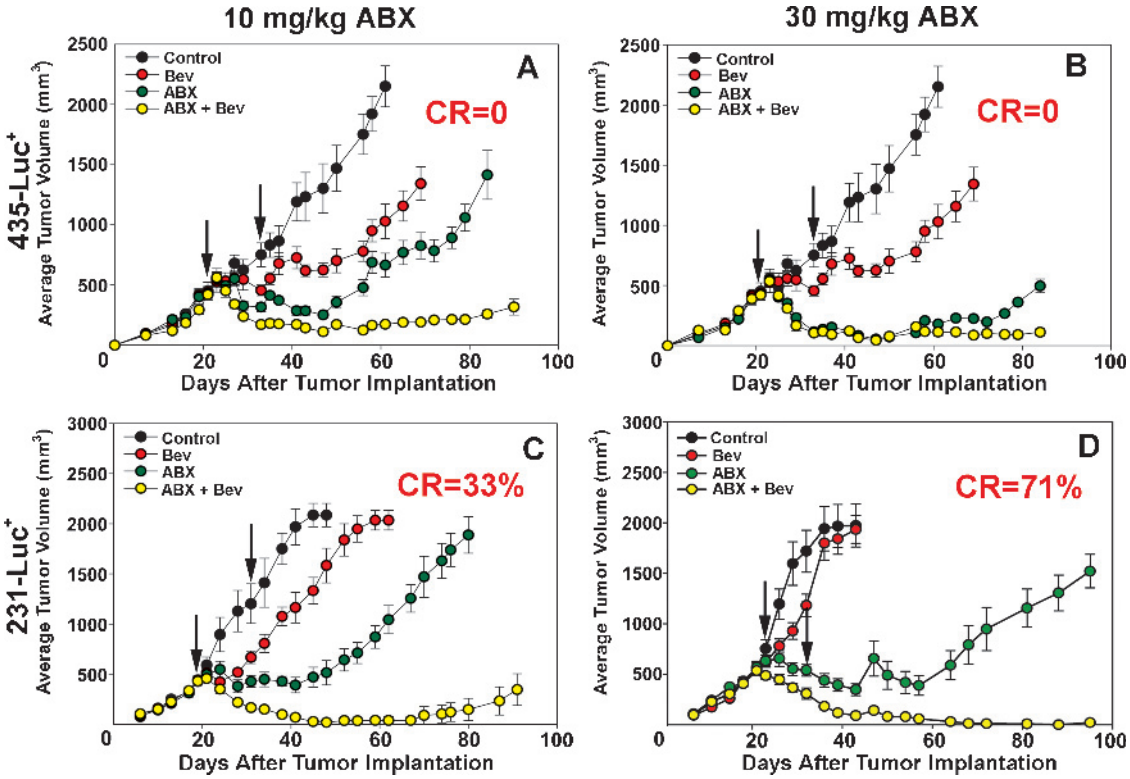

Figure 2. Combined bevacizumab and nab-paclitaxel therapy enhances tumor growth inhibition in mice with orthotopic advanced tumors. Mice were orthotopically implanted with 435-Luc$^+$ (A, B) or 231-Luc$^+$ (C, D) tumors and grown to an average tumor volume of 450 to 600 mm^3. Tumor-bearing mice undergoing monotherapies were treated with bevacizumab (4 mg/kg, two cycles) (A–D), nab-paclitaxel (10 mg/kg, daily for five consecutive days cycle) (A and C), or nab-paclitaxel (30 mg/kg, daily for five consecutive days) (B and D). Combined treatment with bevacizumab and 10 or 30 mg/kg of nab-paclitaxel (daily for five consecutive days for two courses) consisted of i.p. injections of bevacizumab biweekly starting 24 hours after the first nab-paclitaxel injection for the duration of the study. Black arrows in all panels indicate the start of each cycle. The red CR corresponds to the percentage of CRs in the combination group. Each group consisted of 7 to 16 mice. Data are presented as the mean tumor volume ± SE per group at the indicated days after implantation.

231-Luc$^+$ tumors in 71% of the mice. The treatment was well tolerated with no mortality or morbidity observed in any of the treated mice (approximately 130 mice in total). These data show in two orthotopic models that the combined nab-paclitaxel/bevacizumab therapy is effective against advanced breast tumors.

Nab-paclitaxel/Bevacizumab Therapy Caused Regression of Existing Metastases in Advanced BC Models

Metastases is the main cause of mortality from cancer [34]. Because the combined therapy was highly efficacious against advanced primary tumors, we sought to determine its effect on metastases in the same models. The 231-Luc$^+$ tumors disseminate primarily through lymphatics [30], whereas 435-Luc$^+$ tumors undergo mainly hematogenous metastasis [16,35]. Thus, analysis in these two models allows for assessment of the antimetastatic efficacy in tumors disseminating through either route. To this end, mice with tumors of 450 to 600 mm^3 in volume (7-16 mice per group) were treated with saline, 10 or 30 mg/kg of nab-paclitaxel alone or combined with bevacizumab (4 mg/kg). Mice were killed when control tumors reached 1800 mm^3, followed by measurement of luciferase activity in LN and lung extracts to quantify incidence and metastatic burden, as previously described [16,30].

In the 435-Luc$^+$ model, positive LN and pulmonary metastases were detected in 12.5% and 100% of control mice, respectively (Figure 3*A*). Bevacizumab alone had no effect on either LN or lung metastasis, whereas nab-paclitaxel alone increased, rather than decreased, both incidence and burden of LN metastases (Figure 3, *A* and *B*). The incidence was raised from 12.5% in the control group to 75% in the group treated by nab-paclitaxel at does of 10 mg/kg (P = .041). A similar trend was detected in mice treated with 30 mg/kg (25% higher than control; Figure 3*A*). Importantly, combination therapy suppressed both incidence and LN metastatic burden by reducing it to basal or below basal level. For instance, in mice treated with 10 mg/kg, the mean luciferase activity in LN decreased from 194,126 ± 47,252 RLU/mg protein in chemotherapy-alone group to 0 ± 0 RLU/mg in the combination group (P < .001).

With regard to lung metastasis in the 435-Luc$^+$ model, neither incidence nor burden was affected by a single nab-paclitaxel treatment. However, when nab-paclitaxel at the dose of 10 mg/kg was combined with bevacizumab, the incidence and burden of lung metastasis were reduced by 57% and 93%, respectively (Figure 3, *A* and *B*). This result was statistically significant (P = .026) compared with either control or nab-paclitaxel alone group (Figure 3*B*). The combination group treated with 30 mg/kg of nab-paclitaxel showed a similar trend in reduction of incidence, but the values did not reach statistical significance.

The effect on LN metastasis was of major interest in this study because it is well established that lymphatic vessels are the primary route for dissemination of BCs [36]. As we previously described [16] and show here (Figure 1), orthotopically implanted 231-Luc$^+$ breast

carcinoma line is an excellent model for human BC because it demonstrates 100% incidence of LN metastases in untreated mice. On the basis of the Fisher exact test, the incidence of LN metastasis was not significantly affected by monotherapy with bevacizumab or nab-paclitaxel administrated at either the 10- or the 30-mg/kg dose (Figure 3*C*, *left panel*). However, the metastatic burden in LN was reduced in groups treated with bevacizumab alone ($P = .005$) as well as in groups treated with 10 and 30 mg/kg nab-paclitaxel ($P = .003$ and

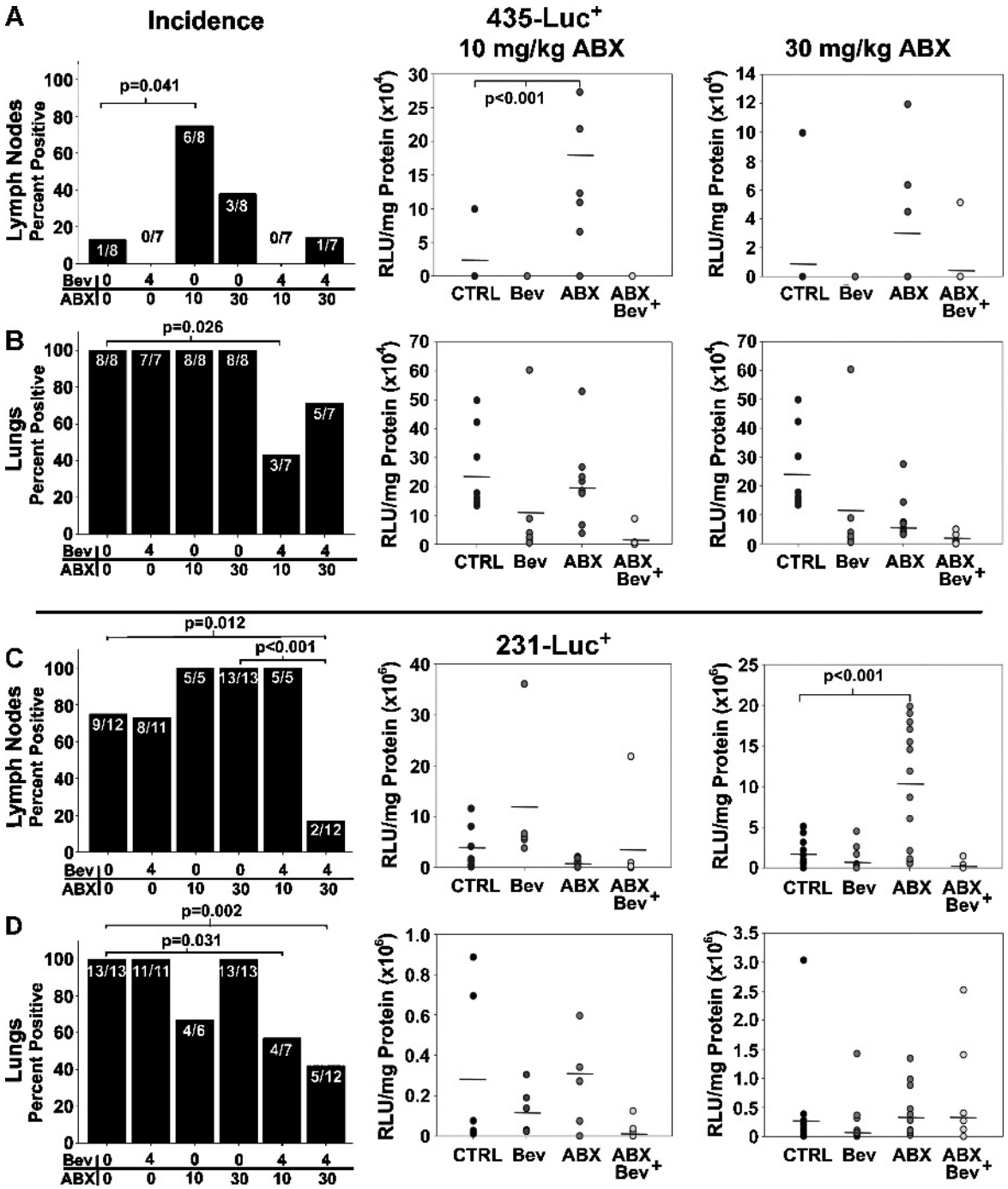

Figure 3. Bevacizumab suppresses antimetastatic effects of nab-paclitaxel therapy in mice with advanced tumors. Metastasis to the LNs and lungs was assessed in mice bearing advanced orthotopic 435-Luc$^+$ (A and B) and 231-Luc$^+$ (C and D) tumors after monotherapy with 10 or 30 mg/kg nab-paclitaxel or combined with bevacizumab administrated at 4 mg/kg. Each group consisted of 7 to 16 mice. Metastatic burden was measured by luciferase activity normalized to total milligrams of protein in lysates from axillary, brachial, inguinal LNs, and one lobe of the lung. Metastatic incidence in the LNs and lungs is represented in the left panel in A, B, C, and D. Data presented at the center and right panels are the metastatic burden of the LNs and lungs treated with 10 or 30 mg/kg ABX, respectively. Metastatic burden of individual mice is represented by the dots, and the black bars indicate the average metastatic burden ± SE per group. Statistical significance was assessed by Fisher exact test and Wilcoxon rank sum test for incidence and burden, respectively. *P* values shown black represent statistically significant changes in incidence or metastatic burden.

P = .001, respectively). Importantly, the combination therapy consisting of 30 mg/kg of nab-paclitaxel and bevacizumab eradicated both LN and lung metastases in 83% (10/12) and 58% (7/12) of the mice (n = 12 per group). These results were highly statistically significant compared with either control (P < .002) or 30 mg/kg of nab-paclitaxel alone group (P < .001 and P < .002 for inhibition of LN and lung metastasis, respectively). To assess whether the antimetastatic effect of the combined nab-paclitaxel and bevacizumab therapy was additive or synergistic, we used the CompuSyn software described in the Materials and Methods. The analysis determined a confidence interval less than 0.001 for the effect of the combination therapy on LN metastasis, demonstrating that this effect is highly synergistic compared with nab-paclitaxel or bevacizumab alone. The effects on lung metastasis did not reach synergistic level, possibly because of the relatively low metastatic burden in the lungs at the time of analysis of this model.

In summary, the nab-paclitaxel/bevacizumab therapy showed significantly improved antimetastatic efficacy in both models of advanced 435-Luc$^+$ and 231-Luc$^+$. The combined therapy was the least efficacious against lung metastasis in the 435-Luc$^+$ model, resulting in a reduced incidence by 29% compared with nab-paclitaxel treated mice. The combined therapy was the most efficacious against LN metastasis in the 231-Luc$^+$ model, resulting in 83% and 92% reduction in incidence and burden, respectively, whereas the monotherapy of either drug was ineffective.

Effect of Sequence of Drugs' Administration on Efficacy of Combined Therapy

The optimal schedule for sequence of nab-paclitaxel/bevacizumab administration was determined in the 435-Luc$^+$ tumor model because this model was more responsive to bevacizumab. Mice bearing 450 mm^3-sized 435-Luc$^+$ tumors were treated with saline (control; group 1) or with nab-paclitaxel (10 mg/kg) and bevacizumab (4 mg/kg) using three distinct regimens outlined in Figure 4*A*. Group 2 received bevacizumab immediately after cessation of nab-paclitaxel treatment. Group 3 received the antibody concurrently with nab-paclitaxel, and both drugs were terminated simultaneously. Group 4 also received both drugs concurrently, but the bevacizumab therapy continued until the last day of the experiment (118 days).

The results showed that the sequential regimen (group 2) was the least efficacious, suppressing tumor growth by 80% compared with 95% and 98% inhibition in groups 3 and 4, respectively (Figure 4*B*). The superior outcome after concurrent cytotoxic/anti–VEGF-A therapy suggested that VEGF-A is elevated immediately on initiation of therapy and plays an important role in chemoresistance. This hypothesis was supported by comparison of VEGF-A expression in control- and nab-paclitaxel– (10 mg/kg) treated tumors harvested at days 0 to 8 after treatment. Tumors harvested 3 to 5 days after treatment showed significant dose-dependent increases in VEGF-A expression in treated but not in control tumors. Quantitative analysis performed using the ImageJ software showed widespread VEGF-A increase detected in all treated but not the control tumors (Figures 4, *C* and *D*, and W1). This suggests that, for optimal results, anti–VEGF-A antibody and chemotherapy should be administrated concurrently.

Basis for Synergistic Effect of Nab-paclitaxel and Bevacizumab Therapy

We next sought to determine the mechanisms underlying the synergistic effects of combined therapy. Paclitaxel and nab-paclitaxel have been previously shown to induce expression of VEGF-A in tumor cells *in vitro* [16,37]. Figure 4 shows that nab-paclitaxel also induces VEGF-A tumor cells *in vivo*. VEGF-A counteracts the efficacy of cytotoxic drugs by promoting tumor cell survival [16]. This effect might be mediated through VEGF-A–dependent activation of the NF-κB pathway [37] that upregulates numerous proteins essential for cell survival [38]. This mechanism might account for a significantly better outcome observed in combination groups.

To test this hypothesis, we first determined activation of the NF-κB pathway by nab-paclitaxel in cultured 231-Luc$^+$ cells. Cells were treated with escalating doses of nab-paclitaxel (0-30 nM) for 8 to 48 hours followed by Western blot analysis. Eight hours after exposure to nab-paclitaxel, the expression of phosphorylated p-p50 and p-p65 subunits of the NF-κB as well as Bcl-xL was significantly increased (Figure 5*A*). Later time points (24 and 48 hours) showed significant increases in p-Akt and p-p44/42, although the expression of nonphosphorylated counterparts remained unchanged (Figures 5*A* and W2). NF-κB activation by nab-paclitaxel was further confirmed by measuring inflammatory cytokines IL-6 and IL-8, the downstream products of this pathway. Cytokines from the conditioned medium of 231-Luc$^+$ cells treated for 72 hours with nab-paclitaxel (2.5-30 nM) were measured using Luminex. Nab-paclitaxel significantly increased expression of both IL-6 and IL-8 in a dose-dependent manner up to maximum of 20- to 22-fold (Figure 5*B*). TNF-α was also increased from undetectable level to 9.5×10^3 pg normalized per 1×10^6 cells (Figure 5*C*). These findings demonstrate that nab-paclitaxel activates the NF-κB pathway in tumor cells leading to increased expression of IL-6, IL-8, TNF-α, Bcl-2, and Bcl-xL, all of which may trigger reactionary angiogenesis [39] and promote survival of tumor cells [38].

We next determine whether nab-paclitaxel behaves similarly *in vivo*. Groups of 231-Luc$^+$–bearing mice (n = 4) with advanced tumors (500 mm^3) were treated with nab-paclitaxel (30 mg/kg) followed by analysis on the third, fifth, and eighth days after initiation of the treatment. Tumor lysates and sections were analyzed for the expression of NF-κB and prosurvival proteins using Western blot and immunohistochemistry, respectively. The expression of several inflammatory and prosurvival proteins including p-p50, p-p44/42, p-Akt, Bcl-2, and Bcl-xL has significantly increased after nab-paclitaxel treatment. The highest increase for most targets was on the eighth day after treatment (Figures 6*A* and W3). Of all targets, up-regulation of Bcl-2 and Bcl-xL was the most conspicuous, and these targets were confirmed by immunohistochemistry. Control tumors displayed homogenous but weak Bcl-2 expression and strong but sporadically expressed Bcl-xL (Figure 6*B*, *Control*). Three days after nab-paclitaxel treatment, the expression of both proteins was slightly decreased or unchanged. However, at the fifth and eighth days after treatment, the expression of both proteins was significantly increased (Figure 6*B*). Collectively, these data suggest that chemotherapy-induced expression of VEGF-A followed by activation of the NF-κB pathway play an important role in chemoresistance of advanced tumors.

Discussion

This study demonstrates that combination of nab-paclitaxel and bevacizumab is highly efficacious against advanced orthotopic breast tumor xenografts and preexisting lymphatic and visceral metastases. The improved efficacy of combined therapy was demonstrated by substantial tumor suppression, delayed time to progression, and, in

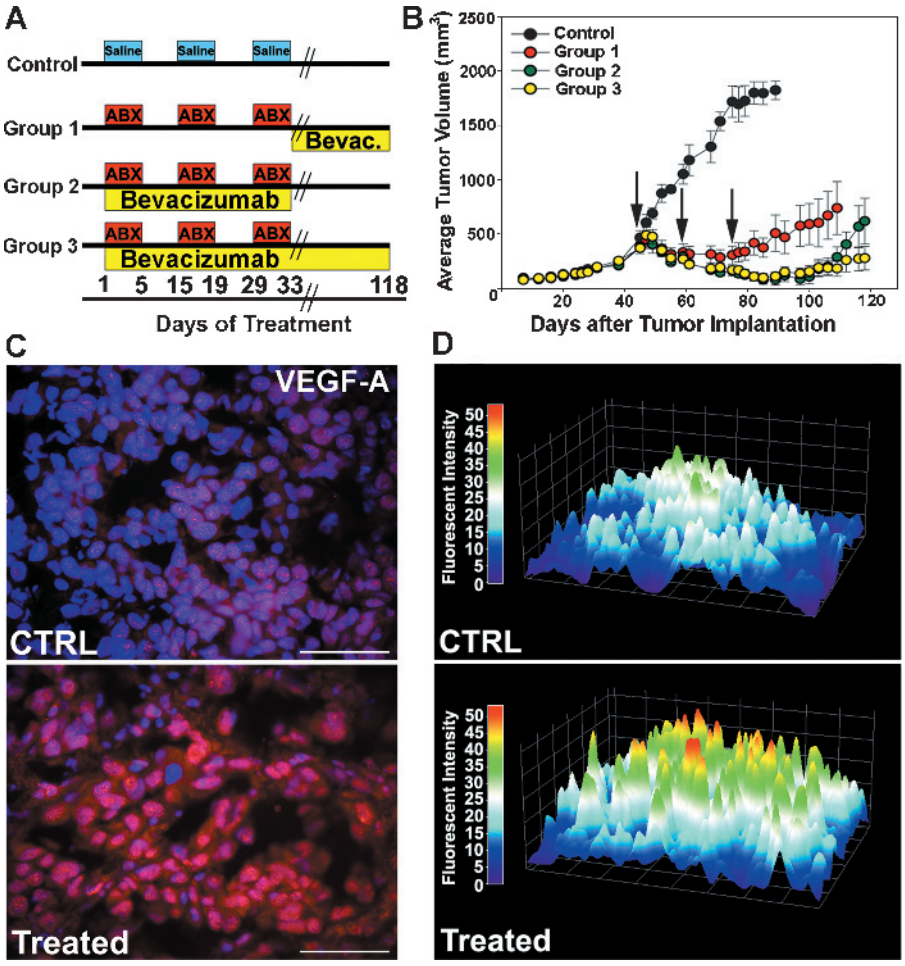

Figure 4. Bevacizumab treatment concurrent with nab-paclitaxel chemotherapy is the most effective regimen for inhibiting tumor growth and metastasis. (A, B) Mice bearing 435-Luc$^+$ tumors of 450 mm^3 in volume were treated with bevacizumab (4 mg/kg) using three different combination regimens with nab-paclitaxel (10 mg/kg, three cycles of daily for five consecutive days). (A) Schematic illustration of experimental design describing different regimens assessed in this study. Group 1 received three cycles of nab-paclitaxel followed by bevacizumab for the duration of the study, group 2 received bevacizumab concurrent with nab-paclitaxel and both drugs were discontinued at the end of three cycles of nab-paclitaxel, and group 3 received bevacizumab throughout three cycles of nab-paclitaxel and for the duration of the study. (B) Black arrows indicate the start of each cycle of nab-paclitaxel treatment. Data are presented as the mean tumor volume ± SE per group at the indicated days after implantation. Frozen sections from control- (C, top) and nab-paclitaxel-treated (C, bottom) tumors were stained with anti–VEGF-A antibodies and counterstained with 4′,6-diamidino-2-phenylindole to visualize the nuclei. Images were acquired at a constant exposure setting and total fluorescent intensity of VEGF-A staining from control (D, top) and treated (D, bottom) tumor sections was plotted using the ImageJ software as described in the Materials and Methods. Fluorescent intensity plots of representative images in (C) are shown. All images were acquired at a magnification of ×200.

the 231-Luc$^+$ model, eradication of both large-sized tumors and metastases. These results provide novel evidence for a mechanism underlying the synergy between two drugs. We show that chemoresistance was due to the up-regulation of VEGF-A followed by the activation of the NF-κB pathway in tumor cells leading to the production of inflammatory cytokines and prosurvival proteins that diminish the chemotherapeutic efficacy. These data provide a basis for combining nab-paclitaxel and anti–VEGF-A therapies to sustain therapeutic gains.

The concept of improving efficacy of chemotherapy by combining with antiangiogenic drugs has been previously shown in several studies [16,40]. However, most previous studies were performed in mice with small-sized (100-150 mm^3) tumors, which precludes direct comparison to our results. We reviewed 65 published studies that assessed chemotherapeutic effects in BC models (Table W1). Only two previous studies challenged mice bearing tumors larger than 400 mm^3 [41,42]. We sought to impart a better realism to xenograft models by delaying the treatment until tumors reached 450 to 600 mm^3. To our knowledge, this is the first report of CR sustainable longer than 100 days occurring in more than 70% of mice bearing advanced (>450 mm^3) orthotopic xenografts. Combination therapy also significantly suppressed advanced 435-Luc$^+$ tumors, although no CRs were observed. This could be due to the genetic differences between 231-Luc$^+$ and 435-Luc$^+$ tumors that would be associated with increased resistance to paclitaxel, survival, or metastatic potential. This is indirectly supported by the propensity of 435-Luc$^+$ tumors to undergo hematogenous metastasis, which requires a superior ability to survive in the bloodstream [43]. Nevertheless, more than 90% suppression of 231-Luc$^+$ and 435-Luc$^+$ advanced tumors and 71% of CR in mice with 231-Luc$^+$ tumors

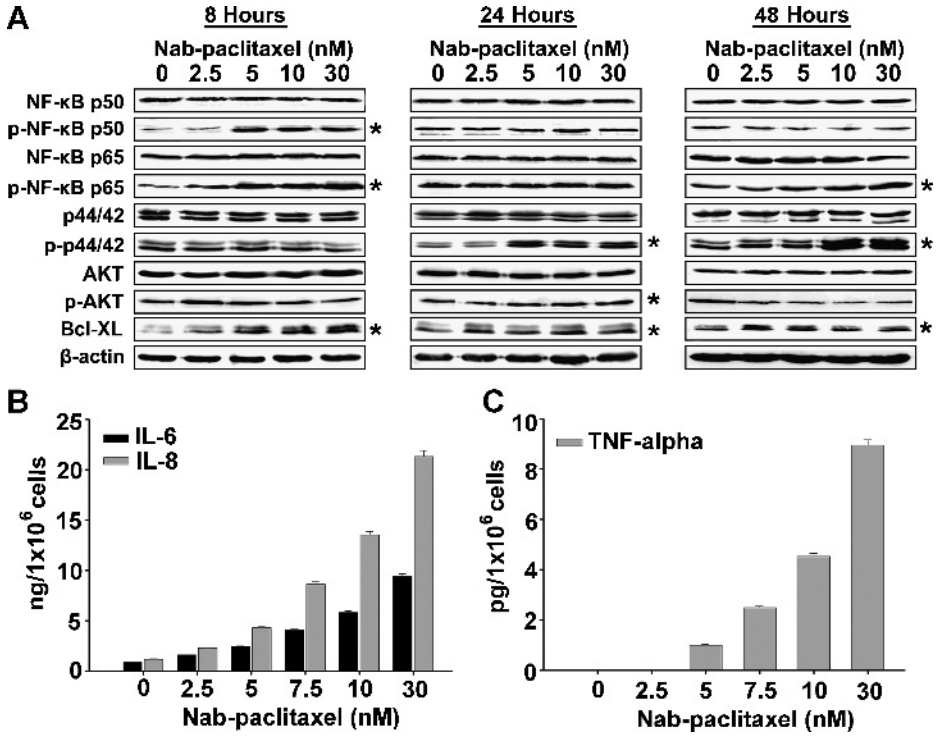

Figure 5. Treatment of breast carcinoma 231-Luc$^+$ cells with nab-paclitaxel induces inflammatory response. (A) 231-Luc$^+$ cells were plated at a density of 2.5 × 10^6 cells per well in six-well plates and treated with a nab-paclitaxel (0-30 nM) for 8 (left), 24 (center), and 48 (right) hours. Control and treated 231-Luc$^+$ cell lysates were analyzed by Western blot for changes in the phosphorylated and nonphosphorylated forms of NF-κB p50, NF-κB p65, Erk p44/42, Akt, and unmodified Bcl-xL. β-Actin served as a loading control. The asterisks represent targets with significant changes in response to nab-paclitaxel treatment. (B, C) Production of inflammatory cytokines by 231-Luc$^+$ cells treated for 72 hours with nab-paclitaxel (0-30 nM) was determined in the conditioned medium by Luminex assay. Note that IL-6 and IL-8 (B) and TNF-α (C) are highly upregulated in response to nab-paclitaxel treatment in a dose-dependent manner. Data are presented as the mean cytokine concentration normalized per number of viable tumor cells that are derived from two independent experiments ± SE.

represent significantly improved outcome in both models than is typically reported for combined Cremophor-based paclitaxel/anti–VEGF-A therapy [17].

Metastatic BC is currently considered incurable [44–46], with a median survival of 18 to 24 months [45], and palliative treatment is offered as the only option [46]. We show that the combined nab-paclitaxel/bevacizumab therapy significantly suppressed or eradicated *preexisting* lymphatic and pulmonary metastases in mice bearing 450 to 600 mm^3 human breast xenografts. Eradication of preexisting metastases demonstrated in these orthotopic advanced BC models

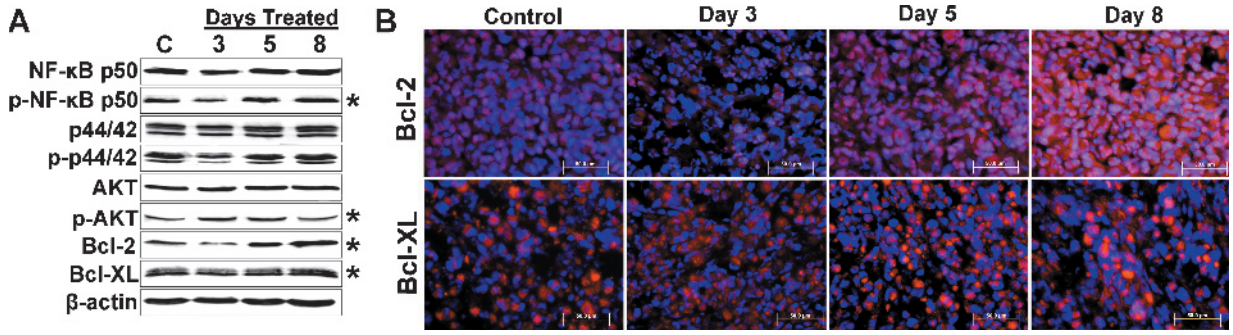

Figure 6. Nab-paclitaxel therapy activates prosurvival and inflammatory pathways in advanced orthotopic 231-Luc$^+$ tumors *in vivo*. Mice bearing orthotopic 231-Luc$^+$ tumors of equal or higher than 500 mm^3 in volume were treated with daily injection of 30 mg/kg of nab-paclitaxel for 3, 5, and 8 days. (A) Western blot analysis of the expression of phosphorylated and nonphosphorylated forms of NF-κB p50, p44/42, Akt, and unmodified Bcl-2 and Bcl-xL in mixed lysates from tumors harvested on days 3, 5, and 8 after the beginning of treatment (n = 4 mice per group). β-Actin was used as a loading control. Note upregulated expression of p-p50, p-Akt, Bcl-2, and Bcl-xL as indicated by the asterisks. (B) Frozen tumor sections from mice treated with nab-paclitaxel for 3, 5, and 8 days were stained with antibodies against prosurvival proteins, Bcl-2 (top row) and Bcl-xL (bottom row). The center of all treated tumors was highly necrotic and devoid of positive staining for any targets. All images were acquired at 200× magnification from the margins of the tumor. Note the significant time-dependent increase in the expression of both Bcl-2 and Bcl-xL after 3 to 8 days of nab-paclitaxel treatment.

challenges the current dogma of incurability of metastasis and suggests that this strategy may cure patients with advanced metastatic disease.

The ability of anti–VEGF-A antibody to suppress the prometastatic effect of chemotherapy suggests that VEGF-A is primarily responsible for the paclitaxel-induced prosurvival effects. Nab-paclitaxel–dependent induction of VEGF-A has been previously demonstrated in our studies [16] and confirmed by other groups [37]. Currently, the mechanisms leading to VEGF-A up-regulation by paclitaxel and the consequences of VEGF-A signaling for tumor recurrence are poorly understood. We hypothesized that chemotherapy-induced VEGF-A might also participate in the hyperactivation of the NF-κB pathway in tumor cells as well as being a product of NF-κB activation. We show here that exposure to nab-paclitaxel correlates with activation of the NF-κB as demonstrated by the overexpression of its target inflammatory and prosurvival proteins including IL-6, IL-8, TNFα, Bcl-2, and Bcl-xL (Figures 5 and 6). This is consistent with a wealth of reported evidence demonstrating NF-κB activation in tumor cells by various chemotherapeutic drugs including Cremophor-based paclitaxel [47–49]. Paclitaxel-dependent increased expression of NF-κB–dependent inflammatory [47] and prosurvival proteins [49] has been widely reported in various tumor lines. NF-κB activation in tumor lines has been shown to correlate with the up-regulation of VEGF-A [9,16], p-Akt [49], Bcl-2, and Bcl-xL [50]; increased tumor cell survival [51]; metastasis [52]; and resistance to chemotherapy [51]. Our data show that nab-paclitaxel is similar to Taxol and other cytotoxic drugs with regard to increasing the functional capacity of the NF-κB and its consequences for tumor progression. On the basis of these reports and the data presented here, we postulate that the tumor-promoting effects of nab-paclitaxel, including resistance to apoptosis and increase in metastasis, are due to VEGF-A–induced and NF-κB–mediated signaling that prevents cytotoxic cell death whereby resisting chemotherapy. Consequently, depletion of VEGF-A concurrently with chemotherapy eliminates the first stimulus for NF-κB activation, thus permitting the full potential of a cytotoxic drug to materialize.

Conclusions

In summary, we show here that nab-paclitaxel/bevacizumab therapy eradicates large orthotopic breast tumors and preexisting LN and pulmonary metastases. The optimal results were achieved by concurrent but not sequential bevacizumab administration, implicating VEGF-A as an immediate response factor for resistance to chemotherapy. Low doses of chemotherapy were largely ineffective against advanced primary tumors and occasionally increase metastases. The mechanism of resistance to nab-paclitaxel involves activation of the NF-κB pathway in malignant cells that increased production of inflammatory mediators and prosurvival Bcl-2 and Bcl-xL proteins. This study suggests that two major factors in prevention of tumor recurrence are efficient delivery of cytotoxic drugs and concurrent suppression of chemotherapy-activated prosurvival traits endowed by VEGF-A initiated activation of the NF-κB pathway. The high efficacy of this approach against large metastatic BC xenografts strongly advocates for adapting nab-paclitaxel/bevacizumab regimen in the clinics.

Acknowledgments

The authors thank Rita Trammel for performing LincoPlex analysis of cytokine production and Abraxis Health for providing nab-paclitaxel for this study.

References

[1] Alassas M, Chu Q, Burton G, Ampil F, Mizell J, and Li BD (2005). Neoadjuvant chemotherapy in stage III breast cancer. *Am Surg* **71**, 487–492.

[2] Rossi D, Baldelli AM, Casadei V, Fedeli SL, Alessandroni P, Catalano V, Giordani P, Ceccolini M, Graziano F, and Catalano G (2008). Neoadjuvant chemotherapy with low dose of PEGylated liposomal doxorubicin plus weekly paclitaxel in operable and locally advanced breast cancer. *Anticancer Drugs* **19**, 733–737.

[3] Bristol IJ, Woodward WA, Strom EA, Cristofanilli M, Domain D, Singletary SE, Perkins GH, Oh JL, Yu TK, Terrefe W, et al. (2008). Locoregional treatment outcomes after multimodality management of inflammatory breast cancer. *Int J Radiat Oncol Biol Phys* **72**, 474–484.

[4] Atalay C, Deliloglu Gurhan I, Irkkan C, and Gunduz U (2006). Multidrug resistance in locally advanced breast cancer. *Tumour Biol* **27**, 309–318.

[5] Ferrara N (2005). VEGF as a therapeutic target in cancer. *Oncology* **69**(suppl 3), 11–16.

[6] Ferrara N, Hillan KJ, and Novotny W (2005). Bevacizumab (Avastin), a humanized anti-VEGF monoclonal antibody for cancer therapy. *Biochem Biophys Res Commun* **333**, 328–335.

[7] Liang Y, Brekken RA, and Hyder SM (2006). Vascular endothelial growth factor induces proliferation of breast cancer cells and inhibits the anti-proliferative activity of anti-hormones. *Endocr Relat Cancer* **13**, 905–919.

[8] McDaid HM, Lopez-Barcons L, Grossman A, Lia M, Keller S, Perez-Soler R, and Horwitz SB (2005). Enhancement of the therapeutic efficacy of taxol by the mitogen-activated protein kinase kinase inhibitor CI-1040 in nude mice bearing human heterotransplants. *Cancer Res* **65**, 2854–2860.

[9] Wild R, Dings RP, Subramanian I, and Ramakrishnan S (2004). Carboplatin selectively induces the VEGF stress response in endothelial cells: potentiation of antitumor activity by combination treatment with antibody to VEGF. *Int J Cancer* **110**, 343–351.

[10] Tsuchida R, Das B, Yeger H, Koren G, Shibuya M, Thorner PS, Baruchel S, and Malkin D (2008). Cisplatin treatment increases survival and expansion of a highly tumorigenic side-population fraction by upregulating VEGF/Flt1 autocrine signaling. *Oncogene* **28**, 3923–3934.

[11] Riedel F, Gotte K, Goessler U, Sadick H, and Hormann K (2004). Targeting chemotherapy-induced VEGF up-regulation by VEGF antisense oligonucleotides in HNSCC cell lines. *Anticancer Res* **24**, 2179–2183.

[12] Lev DC, Ruiz M, Mills L, McGary EC, Price JE, and Bar-Eli M (2003). Dacarbazine causes transcriptional up-regulation of interleukin 8 and vascular endothelial growth factor in melanoma cells: a possible escape mechanism from chemotherapy. *Mol Cancer Ther* **2**, 753–763.

[13] Mills PJ, Parker B, Jones V, Adler KA, Perez CJ, Johnson S, Cohen-Zion M, Marler M, Sadler GR, Dimsdale JE, et al. (2004). The effects of standard anthracycline-based chemotherapy on soluble ICAM-1 and vascular endothelial growth factor levels in breast cancer. *Clin Cancer Res* **10**, 4998–5003.

[14] Huang Y and Fan W (2002). IκB kinase activation is involved in regulation of paclitaxel-induced apoptosis in human tumor cell lines. *Mol Pharmacol* **61**, 105–113.

[15] Bischof M, Abdollahi A, Gong P, Stoffregen C, Lipson KE, Debus JU, Weber KJ, and Huber PE (2004). Triple combination of irradiation, chemotherapy (pemetrexed), and VEGFR inhibition (SU5416) in human endothelial and tumor cells. *Int J Radiat Oncol Biol Phys* **60**, 1220–1232.

[16] Volk LD, Flister MJ, Bivens CM, Stutzman A, Desai N, Trieu V, and Ran S (2008). Nab-paclitaxel efficacy in the orthotopic model of human breast cancer is significantly enhanced by concurrent anti–vascular endothelial growth factor A therapy. *Neoplasia* **10**, 613–623.

[17] Gerber HP and Ferrara N (2005). Pharmacology and pharmacodynamics of bevacizumab as monotherapy or in combination with cytotoxic therapy in preclinical studies. *Cancer Res* **65**, 671–680.

[18] Cohn DE, Valmadre S, Resnick KE, Eaton LA, Copeland LJ, and Fowler JM (2006). Bevacizumab and weekly taxane chemotherapy demonstrates activity in refractory ovarian cancer. *Gynecol Oncol* **102**, 134–139.

[19] Sandler AB, Johnson DH, and Herbst RS (2004). Anti–vascular endothelial growth factor monoclonals in non–small cell lung cancer. *Clin Cancer Res* **10**, 4258s–4262s.

[20] de Gramont A and Van Cutsem E (2005). Investigating the potential of bevacizumab in other indications: metastatic renal cell, non–small cell lung, pancreatic and breast cancer. *Oncology* **69**(suppl 3), 46–56.

[21] Miller KD (2003). E2100: a phase III trial of paclitaxel *versus* paclitaxel/bevacizumab for metastatic breast cancer. *Clin Breast Cancer* **3**, 421–422.

[22] Damascelli B, Cantu G, Mattavelli F, Tamplenizza P, Bidoli P, Leo E, Dosio F, Cerrotta AM, Di Tolla G, Frigerio LF, et al. (2001). Intraarterial chemotherapy

with polyoxyethylated castor oil free paclitaxel, incorporated in albumin nanoparticles (ABI-007): phase II study of patients with squamous cell carcinoma of the head and neck and anal canal: preliminary evidence of clinical activity. *Cancer* **92**, 2592–2602.

[23] Ibrahim NK, Desai N, Legha S, Soon-Shiong P, Theriault RL, Rivera E, Esmaeli B, Ring SE, Bedikian A, Hortobagyi GN, et al. (2002). Phase I and pharmacokinetic study of ABI-007, a Cremophor-free, protein-stabilized, nanoparticle formulation of paclitaxel. *Clin Cancer Res* **8**, 1038–1044.

[24] Green MR, Manikhas GM, Orlov S, Afanasyev B, Makhson AM, Bhar P, and Hawkins MJ (2006). Abraxane(R), a novel Cremophor(R)-free, albumin-bound particle form of paclitaxel for the treatment of advanced non–small-cell lung cancer. *Ann Oncol* **8**, 1263–1268.

[25] ABI 007. *Drugs R D* **4**, 303–305.

[26] Desai N, Trieu V, Yao Z, Louie L, Ci S, Yang A, Tao C, De T, Beals B, Dykes D, et al. (2006). Increased antitumor activity, intratumor paclitaxel concentrations, and endothelial cell transport of Cremophor-free, albumin-bound paclitaxel, ABI-007, compared with Cremophor-based paclitaxel. *Clin Cancer Res* **12**, 1317–1324.

[27] Gradishar WJ, Tjulandin S, Davidson N, Shaw H, Desai N, Bhar P, Hawkins M, and O'Shaughnessy J (2005). Phase III trial of nanoparticle albumin-bound paclitaxel compared with polyethylated castor oil–based paclitaxel in women with breast cancer. *J Clin Oncol* **23**, 7794–7803.

[28] Foote M (2007). Using nanotechnology to improve the characteristics of antineoplastic drugs: improved characteristics of nab-paclitaxel compared with solvent-based paclitaxel. *Biotechnol Annu Rev* **13**, 345–357.

[29] Henderson IC and Bhatia V (2007). Nab-paclitaxel for breast cancer: a new formulation with an improved safety profile and greater efficacy. *Expert Rev Anticancer Ther* **7**, 919–943.

[30] Whitehurst B, Flister MJ, Bagaitkar J, Volk L, Bivens CM, Pickett B, Castro-Rivera E, Brekken RA, Gerard RD, and Ran S (2007). Anti–VEGF-A therapy reduces lymphatic vessel density and expression of VEGFR-3 in an orthotopic breast tumor model. *Int J Cancer* **121**, 2181–2191.

[31] Espana L, Fernandez Y, Rubio N, Torregrosa A, Blanco J, and Sierra A (2004). Overexpression of Bcl-xL in human breast cancer cells enhances organ-selective lymph node metastasis. *Breast Cancer Res Treat* **87**, 33–44.

[32] Chou TC, Motzer RJ, Tong Y, and Bosl GJ (1994). Computerized quantitation of synergism and antagonism of taxol, topotecan, and cisplatin against human teratocarcinoma cell growth: a rational approach to clinical protocol design. *J Natl Cancer Inst* **86**, 1517–1524.

[33] Zachary I and Gliki G (2001). Signaling transduction mechanisms mediating biological actions of the vascular endothelial growth factor family. *Cardiovasc Res* **49**, 568–581.

[34] Eccles SA and Welch DR (2007). Metastasis: recent discoveries and novel treatment strategies. *Lancet* **369**, 1742–1757.

[35] Rubio N, Espana L, Fernandez Y, Blanco J, and Sierra A (2001). Metastatic behavior of human breast carcinomas overexpressing the Bcl-x(L) gene: a role in dormancy and organospecificity. *Lab Invest* **81**, 725–734.

[36] Ran S, Volk L, Hall K, and Flister MJ (2009). Lymphangiogenesis and lymphatic metastasis in breast cancer. *Pathophysiology* **17**, 229–251.

[37] Kim HS, Oh JM, Jin DH, Yang KH, and Moon EY (2008). Paclitaxel induces vascular endothelial growth factor expression through reactive oxygen species production. *Pharmacology* **81**, 317–324.

[38] Baldwin AS (2001). Control of oncogenesis and cancer therapy resistance by the transcription factor NF-κB. *J Clin Invest* **107**, 241–246.

[39] Karl E, Warner K, Zeitlin B, Kaneko T, Wurtzel L, Jin T, Chang J, Wang S, Wang CY, Strieter RM, et al. (2005). Bcl-2 acts in a proangiogenic signaling pathway through nuclear factor-κB and CXC chemokines. *Cancer Res* **65**, 5063–5069.

[40] Yang T, Choi MK, Cui FD, Lee SJ, Chung SJ, Shim CK, and Kim DD (2007). Antitumor effect of paclitaxel-loaded PEGylated immunoliposomes against human breast cancer cells. *Pharm Res* **24**, 2402–2411.

[41] Uckun FM, Narla RK, Zeren T, Yanishevski Y, Myers DE, Waurzyniak B, Ek O, Schneider E, Messinger Y, Chelstrom LM, et al. (1998). *In vivo* toxicity, pharmacokinetics, and anticancer activity of Genistein linked to recombinant human epidermal growth factor. *Clin Cancer Res* **4**, 1125–1134.

[42] Ligresti A, Moriello AS, Starowicz K, Matias I, Pisanti S, De Petrocellis L, Laezza C, Portella G, Bifulco M, and Di Marzo V (2006). Antitumor activity of plant cannabinoids with emphasis on the effect of cannabidiol on human breast carcinoma. *J Pharmacol Exp Ther* **318**, 1375–1387.

[43] Mehlen P and Puisieux A (2006). Metastasis: a question of life or death. *Nat Rev Cancer* **6**, 449–458.

[44] Loberg RD, Bradley DA, Tomlins SA, Chinnaiyan AM, and Pienta KJ (2007). The lethal phenotype of cancer: the molecular basis of death due to malignancy. *CA Cancer J Clin* **57**, 225–241.

[45] Miller KD and Sledge GW Jr (2000). High-dose chemotherapy in breast cancer—the perils of history uncontrolled. *Medscape Womens Health* **5**, E1.

[46] Cristofanilli M (2006). Circulating tumor cells, disease progression, and survival in metastatic breast cancer. *Semin Oncol* **33**, S9–S14.

[47] Collins TS, Lee LF, and Ting JP (2000). Paclitaxel up-regulates interleukin-8 synthesis in human lung carcinoma through an NF-κB– and AP-1–dependent mechanism. *Cancer Immunol Immunother* **49**, 78–84.

[48] Liu GH, Wang SR, Wang B, and Kong BH (2006). Inhibition of nuclear factor-κB by an antioxidant enhances paclitaxel sensitivity in ovarian carcinoma cell line. *Int J Gynecol Cancer* **16**, 1777–1782.

[49] Mabuchi S, Ohmichi M, Nishio Y, Hayasaka T, Kimura A, Ohta T, Kawagoe J, Takahashi K, Yada-Hashimoto N, Seino-Noda H, et al. (2004). Inhibition of inhibitor of nuclear factor-κB phosphorylation increases the efficacy of paclitaxel in *in vitro* and *in vivo* ovarian cancer models. *Clin Cancer Res* **10**, 7645–7654.

[50] Chun E and Lee KY (2004). Bcl-2 and Bcl-xL are important for the induction of paclitaxel resistance in human hepatocellular carcinoma cells. *Biochem Biophys Res Commun* **315**, 771–779.

[51] Piva R, Belardo G, and Santoro MG (2006). NF-κB: a stress-regulated switch for cell survival. *Antioxid Redox Signal* **8**, 478–486.

[52] Aggarwal BB, Shishodia S, Takada Y, Banerjee S, Newman RA, Bueso-Ramos CE, and Price JE (2005). Curcumin suppresses the paclitaxel-induced nuclear factor-κB pathway in breast cancer cells and inhibits lung metastasis of human breast cancer in nude mice. *Clin Cancer Res* **11**, 7490–7498.

Table W1. Reported Inhibition of Human Xenografts by Various Regimens Including Chemotherapeutic Drugs Alone or in Combination with Other Antiangiogenic and Other Therapies.

No.	BC Cell Line(s)	TV (mm^3) Before Treatment	Drugs and Doses	Length of Study (d)	% Maximal Inhibition	% CR	PMID
Assessment of combination therapy using paclitaxel and anti-VEGF drugs in various models							
1	MDA-MB-231 Luc$^+$	310	Nab-paclitaxel (10 mg/kg); bevacizumab (4 mg/kg)	110	97	**80***	18516298
2	MDA-MB-231	300	DC101 (2 mg/kg); vinblastin (0.5 mg/kg); adriamycin (1 mg/kg); cisplatin (1-2 mg/kg); cyclosporine A (10 mg/kg); verapmil (20 mg/kg)	130	93	0	11801563
3	MDA-MB-231 and MDA-MB-435	150-200	Cyclophosphamide (10-150 mg/kg); DC101 (800 μg/dose)	120-130	75	0	12019144
4	MCF7	~50	murine 4D5 antibody; rhuMab 4D5 HER-2 antibody (1-3 mg/kg); cisplatin (0.25-0.75 mg/kg); doxorubicin	25	90	0	9811454
5	MX-1	100	Docetaxel (5, 10, or 15 mg/kg); 5-fluorouracil (100 mg/kg); doxorubicin (4 mg/kg); SU11248 (40 mg/kg)	60-90	90	0	14578466
6	GEO	200-300	ZD6474 (150 mg/kg); paclitaxel (20 mg/kg)	100	99	**40**	12684431
7	CWR22R	100-200	rhuαVEGF (5 mg/kg); paclitaxel (6.25 mg/kg)	40	98	0	12374693
8	Hey A8, SKOVip1	100	AEE788 (25 or 50 mg/kg); paclitaxel (75 or 125 mg/kg)	130	95	0	16000591
9	OVCAR3	See below†	Mouse mAb (A4.6.1) (5 μg/g); paclitaxel (20 μg/g)	n/a	83	0	12414537
10	OVCAR3	See below†	VEGF Trap (10 mg/kg); paclitaxel (10 mg/kg)	150	97	0	16203789
11	PC3, A375, A431, A2780, MX-1, HCT116, and MV522	150	JNJ-17029259 (25-125 mg/kg); paclitaxel (30 mg/kg); doxorubicin (3 mg/kg)	60	96	0	15322256
12	PC3-3M-MM2	Palpable	DC101 (1 mg/kg); paclitaxel (0.25 mg/kg)	28	97	0	12171905
13	253J-BV	See below‡	DC101 (1 mg/kg); paclitaxel (10 mg/kg)	56	82	0	10914704
Assessment of chemotherapy and other experimental treatments in breast models							
14	MDA-MB-231, Cal-51 and MCF7	200	Motesanib (75 mg/kg); docetaxel (20 mg/kg); doxorubicin (2.5 mg/kg); tamoxifen (30 mg/kg)	50	66	0	19118038
15	MDA-MB-231, MDA-MB-468, T47D, and MCF7	50-80	Paclitaxel (20 mg/kg)	10-12§	75	0	19239702
16	MDA-MB-231	50-100	F16-IL2 (20 μg), IL-2 (6.6 μg), doxorubicin (1 or 4 mg/kg), paclitaxel (1 or 5 mg/kg)	70-80	90	0	18927291
17	MDA-MB-231	100-150	PEG-Doxorubicin (3 mg/kg) encapsulated in microbubble followed by ultrasound	90	~90	0	17623798
18	MDA-MB-231	150-200	Cyclophosphamide (20 mg/kg); Tirapazamine (25 mg/kg)	85-90	60	0	16452226
19	MDA-MB-231/LM2-4	150-200	UFT (15 mg/kg); cyclophosphamide (20 mg/kg)	46	50	0	16585158
20	MDA-MB-231-H2N	250	Cyclophosphamide (100 mg/kg); Trastuzumab (20 mg/kg)	140	75	0	16467105
21	MDA-MB-231	100	Parthenolide (40 mg/kg) and docetaxel (5 mg/kg)	42§	29	0	15956258
22	MDA-MB-231, BT-474, ZR-75-1	100	AS Bcl-2 and AS Bcl-xL ODNs (5 mg/kg); paclitaxel and docetaxel (10 mg/kg); mitomycin C (2 mg/kg)	36§	90	0	16280040
23	MDA-MB-231	50-100	Diets supplemented with 2%-5% fish or corn oil; doxorubicin (5 mg/kg)	30-35	80	0	12296973
24	MDA-MB-231	100	5-Fluorouracil (30 mg/kg); adriamycin (2.5 mg/kg); TNP-470 (200 mg/kg)	45	15	0	7693335
25	MDA-MB-435	100	Paclitaxel (10 mg/kg); SC144 (25-100 mg/kg)	35	80	0	19322070
26	MDA-MB-435	90-130	Doxorubicin (8 mg/kg)	39	85	0	14696623
27	MDA-MB-435	100-150	RGD (15 or 25 mg/kg); paclitaxel (10 mg/kg)	18§	66	0	18373091
29	MDA-MB-435	100 mg	Docetaxel (25 mg/kg); S-1 (8.3 mg/kg)	25§	67	0	16685389
30	MDA-MB-435	100-200	Adriamycin (5 mg/kg); etoposide (15 mg/kg); salvicine (6-24 mg/kg)	42	83	0	15867248
31	MDA-MB-435	25-50	3G4 (100 μg); docetaxel (10 mg/kg)	35	93	0	15899833
32	MDA-MB-435/LCC6	100-150 g	Bcl-2 AS G3139 and RP ODNs (5 or 10 mg/kg); doxorubicin and liposomal doxorubicin (5 or 10 mg/kg)	70	80	0	10914739
33	MDA-MB-435/LCC6^{MDR1}	See below§	Paclitaxel (12 mg/kg); OC144-093 (30 mg/kg)	35-30§	60	0	10850444
34	MCF7	50-150	Seliciclib (400 mg/kg); doxorubicin (1.5 mg/kg)	18§	70	0	19003963
35	MCF7	Palpable	Lysine (100 mg/kg); RHL (50 or 100 mg/kg); Taxol (10 mg/kg)	35	85	0	19343002
36	MCF7 and MDA-MB-435	100-200	8-quinolinol (20 mg/kg); paclitaxel (15 mg/kg)	60-70	90	0	18506619
37	MCF7	100	Dopamine (50 mg/kg); doxorubicin (5 mg/kg)	14§	37	**14**	18413843
38	MCF7	100	Cisplatin (4, 8 mg/kg); paclitaxel (5, 10 mg/kg); adriamycin (2.3, 4.7 mg/kg)	28§	65	0	18593369
39	MCF7 and MCF7 HER2-18	150-200	Tamoxifen (500 μg/dose); gefitinib (100 mg/kg)	42-56	90	0	18245484
40	MCF7/Dox	100	Doxorubicin (5 mg/kg); 2-methoxyestradiol (30 mg/kg)	28	90	0	18253735
41	MCF7Ca	200	Androstenedione; letrozole	34 weeks	80	0	18559495
42	MCF7	50	Siramesine (6.5 mg/kg); vincristine (30 μg/kg)	14	70	0	17332352
43	MCF7	100-200	PDTC (60 mg/kg); Paclitaxel (10 mg/kg)	35	60	0	17965935
44	MCF7	Palpable	Doxorubicin (5 mg/kg); cyclophosphamide (100 mg/kg)	26	75	0	15667832
45	MCF7^{HER2}	50-100	Trastuzumab (0.03-10 mg/kg); liposomal doxorubicin (1.5-12.5 mg/kg)	50	99	0	15948035
46	MCF7	5-10 mm in diameter	Suramin (10 mg/kg); paclitaxel (15 mg/kg)	90	~90	**50**	15447990
47	MCF7	200	CCI-779 (10 mg/kg); Tamoxifen (500 μg/mouse)	17§	75	0	15585641
48	MCF7 and MDA-MB-468	Tumor mass of 44-68 mg	Dexamethasone (0.1 mg/day); carboplatin (120 mg/kg); gemcitabine (160 mg/kg)	30-70	50	0	15014014
49	Parental MCF7 and various derivatives	50-75	Photress (8, 12, and 18 mg/kg); doxorubicin (8 mg/kg)	—	75	0	15377855

Table W1. (*continued*)

No.	BC Cell Line(s)	TV (mm^3) Before Treatment	Drugs and Doses	Length of Study (d)	% Maximal Inhibition	% CR	PMID
50	MCF7/adr	65	Doxorubicin (4 mg/kg); tetrandrine (30 mg/kg)	32[§]	58	0	11818209
51	MCF7	100	CBR96-doxorubicin (3.3 mg/kg); paclitaxel (10 mg/kg)	35	95	0	11477565
52	MCF7	50-100	Doxorubicin (5 mg/kg); methotrexate (2 mg/kg); VP-16 (20 mg/kg); 5-fluorouracil (16 mg/kg); vinblastine (0.8 mg/kg); cyclophosphamide (80 mg/kg); paclitaxel (15 mg/kg)	25[§]	99	0	10327070
53	MCF7	50-100	Doxorubicin (6 or 8 mg/kg); BR64-doxorubicin (15 mg/kg)	70	87	0	1382845
54	MX-1	50-100	3176152HCl (10 or 30 mg/kg); paclitaxel (24 mg/kg); carboplatin (50 mg/kg)	TGD[¶]	TGD	0	12201487
55	MX-1 and MAXF401	~500	Capecitabine (359 mg/kg); Docetaxel (7.5 mg/kg); 5′dFUrd (123 mg/kg); 5-Fura (13 mg/kg)	84	90	**60**	11309360
56	MX-1	50-100	Cryptophycin 52 (5 mg/kg); cryptophycin 55 (15 mg/kg); doxorubicin (1.75 mg/kg); paclitaxel (24 mg/kg); vionrelbine (7.5 mg/kg); gemcitabine (60 mg/kg); 5-fluorouracil (30 mg/kg)	23 days delay in tumor growth	–	0	10972484
57	MX-1	50	MTA (100, 150, 200 mg/kg); methotrexate (0.8 mg/kg); 5-fluorouracil (30 mg/kg); doxorubicin (1.75 mg/kg); paclitaxel (24 mg/kg)	40	TGD	0	10741729
58	BT474	100-200	Laptinib (30, 60, or 100 mg/kg); topotecan (6 or 10 mg/kg)	75	90	0	19047120
59	SKBR-3	300-500	Edotecarin (3 or 30 mg/kg); docetaxel (5 mg/kg); capecitabine (370 mg/kg)	~50	89	0	17089166
60	BCap37	0.6-0.7 cm in diameter	Dexamethasone (1 mg/kg); paclitaxel (20 mg/kg)	18	93	0	16496381
61	NCI/ADR-RES	100	Evodiamine (10 mg/kg); paclitaxel (20 mg/kg)	75	63	0	15705600
62	KPL-4 and BT-474	100-200	Trastuzumab (15 and 7.5 mg/kg); Capecitabine (126 mg/kg); 5′-dFUrd (43 mg/kg); 5-FUrd (4.6 mg/kg)	35-40	47	0	11935213
63	KPL-4	See below[†]	Docetaxel (5 or 10 mg/kg); 5′-dFUrd (60/kg); tegafur (100 mg/kg)	34	55	0	11710628
64	MDA-MB-468	50-100	Cisplatin (1 mg/kg); doxorubicin (4 mg/kg); p53 adenovirus (8.3×10^8 CIU/dose	25-30	90	0	10412949

*CR percentages higher than 0% are highlighted in bold.
[†]Treatment started 14 days after implantation of tumor cells.
[‡]Treatment started 21 days after implantation of tumor cells.
[§]Tumor burden was assessed by weight.
[¶]Assessed by TGD.

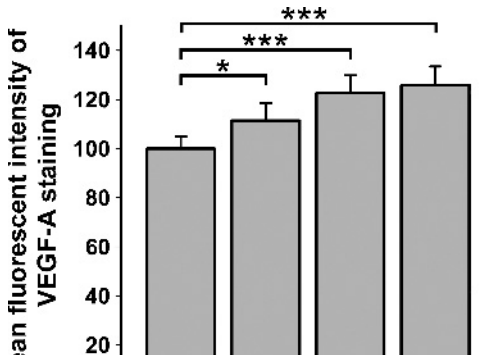

Figure W1. Nab-paclitaxel treatment of 435-Luc$^+$ tumors significantly induces VEGF-A expression. Frozen sections from tumor-bearing mice treated with saline (control) or 10, 20, and 30 ng/ml of nab-paclitaxel were stained with anti–VEGF-A antibodies. The mean fluorescent intensity (MFI) of VEGF-A staining was then calculated using ImageJ software as described in the Materials and Methods. The MFIs of the experimental groups are expressed relative to the MFI detected in tumors from control mice (8.44 ± 0.4 arbitrary units) that was set to a value of 100. Data are presented as the MFI of five independent fields ± SE ($n = 3$ mice per experimental group). *$P < .05$ and ***$P < .001$ *versus* control as determined by Student's t test. Images were acquired at 200× magnification.

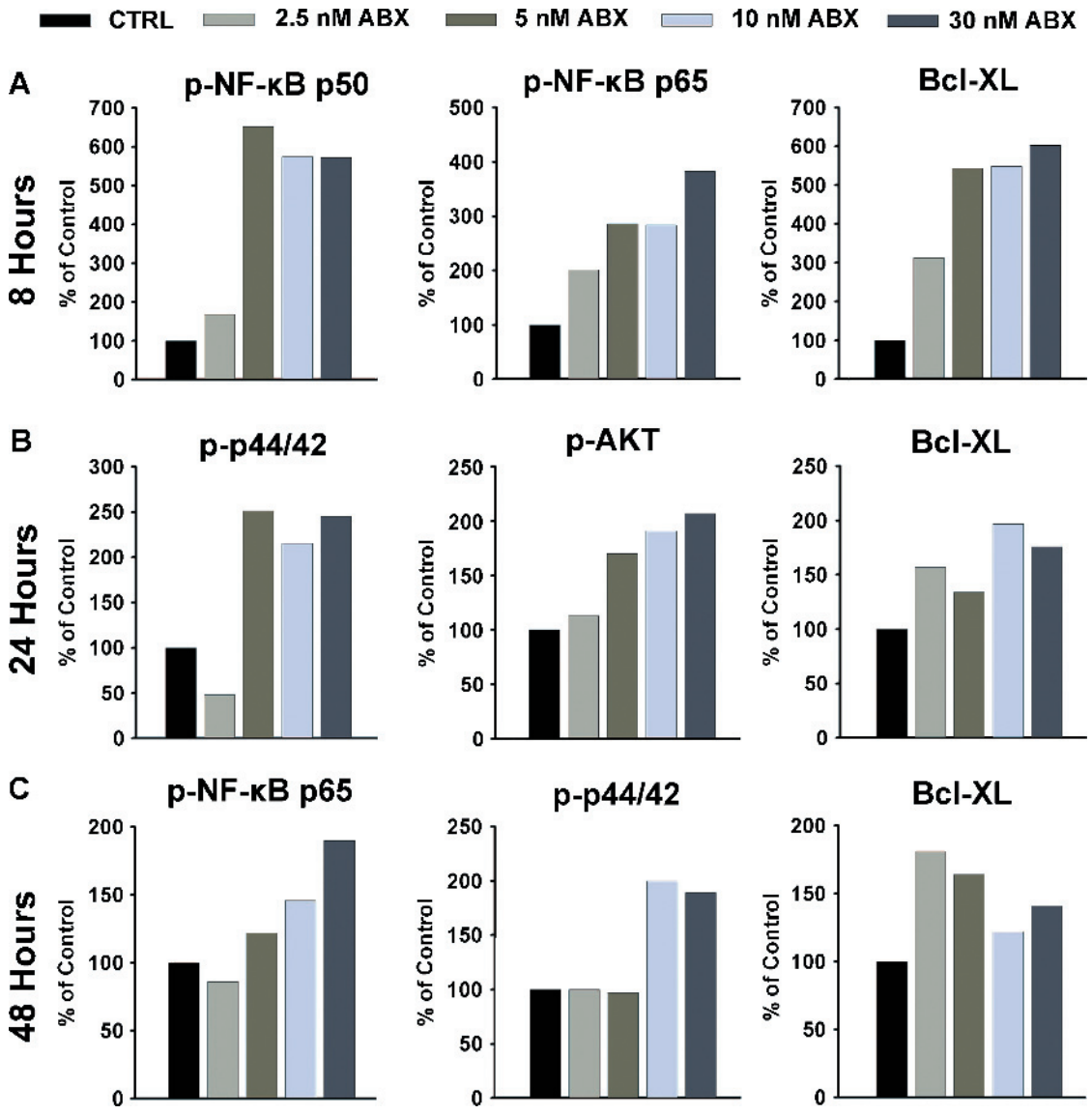

Figure W2. Analysis of elevated prosurvival and inflammatory protein expression induced by nab-paclitaxel treatment of 231-Luc$^+$ cells *in vitro*. Western blots of lysates from cultured 231-Luc$^+$ cells treated for 8 (A), 24 (B), and 48 hours (C) with 0 to 30 nM of nab-paclitaxel (ABX) or PBS (CTRL) were further analyzed by band densitometry using LAS-3000 Image-Reader and Multi Gauge V3.0 software. Only target proteins displaying significant changes in expression by Western blot analysis (Figure 5*A*) were chosen for further analysis as indicated by labels above each graph. Specific concentrations of ABX treatment are also indicated at the top of the figure. Data are presented as percentage of the control 231-Luc$^+$ cell lysates.

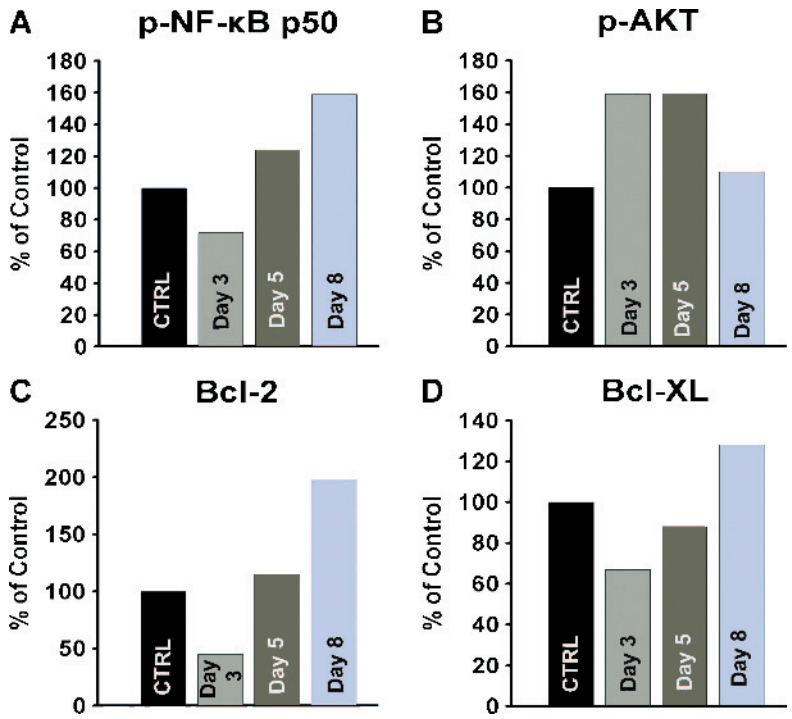

Figure W3. Analysis of highly upregulated prosurvival and inflammatory proteins induced by nab-paclitaxel treatment of 231-Luc$^+$ tumors. Densitometry was performed on Western blots of lysates from 231-Luc$^+$ tumors ~500 mm^3 treated with 30 mg/kg nab-paclitaxel for 2, 4, and 7 days and harvested 24 hours after cessation of each treatment. Shown are analyses of p-NF-κB p50 (A), p-Akt (B), Bcl-2 (C), and Bcl-xL (D) that were detected by Western blot to be highly upregulated by *nab*-paclitaxel treatment compared with saline-treated control mice (Figure 6). Band strength was analyzed as described under the legend for Figure W2, and target protein expression is presented as percentage of protein expression in tumor lysates from control saline-treated mice.